Journal of Applied Polymer Science

Hollow PUA/PSS/Au microcapsules with interdependent near-infrared/pH/temperature multiresponsiveness

Shuhan Xu, Jun Shi, Liu Yang, Qiong Wu, Shaokui Cao
School of Materials Science and Engineering, Zhengzhou University, Zhengzhou 450052, China
Correspondence to: J. Shi (E-mail: shijun@zzu.edu.cn) and S. Cao (E-mail: caoshaokui@zzu.edu.cn)

ABSTRACT: In this work, smart hollow microcapsules made of thermal-/pH-dual sensitive aliphatic poly(urethane-amine) (PUA), sodium poly(styrenesulfonate) (PSS), and Au nanoparticles (AuNPs) for interdependent multi-responsive drug delivery have been constructed by layer-by-layer (LbL) technique. The electrostatic interactions among PUA, PSS, and AuNPs contribute to the successful self-assembly of hollow multilayer microcapsules. Thanks to the shrinkage of PUA above its lower critical solution temperature (LCST) and the interaction variation between PUA and PSS at different pH conditions, hollow microcapsules exhibit distinct pH- and thermal-sensitive properties. Moreover, AuNPs aggregates can effectively convert light to heat upon irradiation with near-infrared (NIR) laser and endow the hollow microcapsules with distinct NIR-responsiveness. More importantly, the NIR-responsive study also demonstrates that the microcapsule morphology and the corresponding NIR-responsive drug release are strongly dependent on the pH value and temperature of the media. The results indicate that the prepared hollow PUA/PSS/Au microcapsules have the great potential to be used as a novel smart drug carrier for the remotely controllable drug delivery. © 2015 Wiley Periodicals, Inc. J. Appl. Polym. Sci. **2016**, *133*, 43008.

KEYWORDS: drug delivery systems; self-assembly; stimuli-sensitive polymers

Received 27 August 2015; accepted 28 September 2015
DOI: 10.1002/app.43008

INTRODUCTION

Stimuli-responsive multilayer microcarriers have attracted significant attention over the past decades.[1,2] Light-responsive microcapsules constructed by layer-by-layer (LbL) self-assembly are widely used in the biomedical field.[3] Compared with the UV or visible light, which has a short tissue penetration depth and is harmful to the human body, the near-infrared (NIR) irradiation to induce the encapsulated material release at the specified location in a remotely controllable manner is quite attractive because most of living organisms and physiological media are relatively transparent to NIR.[4,5] At present, there are some reports concerning the NIR light responsive microcapsules for stimuli-responsive drug release. For example, Wu *et al.* prepared self-propelled polymer multilayer Janus capsules for effective drug delivery and light-triggered release.[6] Hu *et al.* constructed light-responsive gold nanorod-covered kanamycin-loaded hollow SiO_2 nanocapsules for drug delivery and photothermal therapy on bacteria.[7] However, most of them deal with the response to the single NIR light stimulus. Compared with single responsive microcapsules, hollow multilayer microcapsules that can respond to more than one stimulus are more interesting owing to their physiological and biological applications.[8–10] In addition, multiple-responsive microcapsules has a wide selection range of smart responses,[11–13] and the corresponding drug loading efficiency and responsive properties may be improved as well.[14] For example, many studies on NIR single responsive microcapsules have mentioned that the temperature rise upon laser irradiation has a great influence on the NIR-responsive property of the microcapsules.[15] On the other hand, the investigation of NIR-responsiveness at different pH conditions is also necessary because the pH value of tumor is weak acid and the pH value of normal tissue is nearly neutral. Therefore, the design of multiple-responsive microcapsules and the interactive mechanism among different stimuli is very significant to the application of remotely controllable drug delivery.

In the present article, NIR-, pH-, and thermal-responsive properties would be introduced into the hollow polyelectrolyte microcapsules, and the mutual influence among different stimuli has been investigated in detail. To date, a variety of nanoscaled carriers that could absorb NIR light and change light

Additional Supporting Information may be found in the online version of this article.

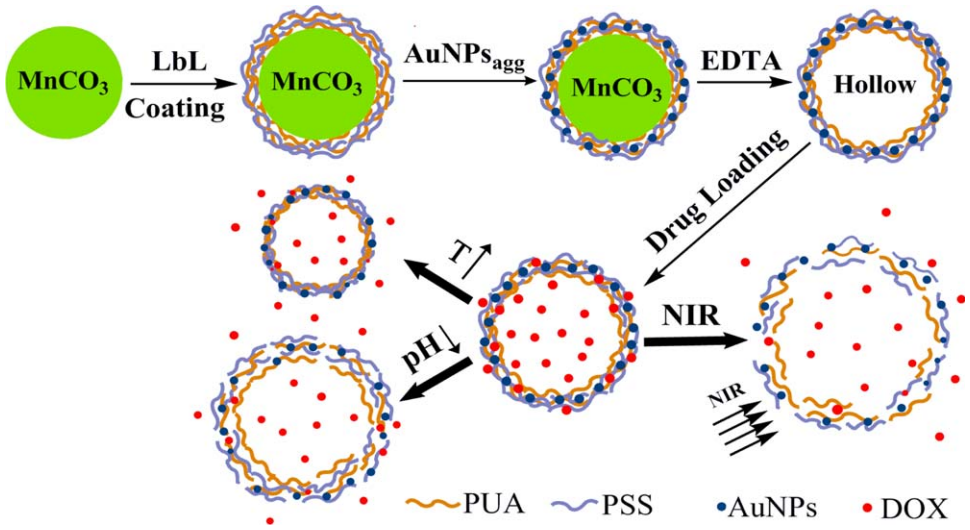

Scheme 1. Schematic illustration of the fabrication for hollow PUA/PSS/Au microcapsules and the near-infrared/pH/temperature-multiple responsive drug delivery from hollow PUA/PSS/Au microcapsules. [Color figure can be viewed in the online issue, which is available at wileyonlinelibrary.com.]

energy into heat energy have been widely employed in thermotherapy.[15] The most widely used are nanogolds, including spherical Au nanoparticles (AuNPs),[16–18] core/shell nanoparticles,[19] hollow Au nanocages,[20] and Au nanorods.[21–23] Compared with other nanostructures, spherical AuNPs have been employed successfully in biomedical application such as drug release or photothermal destruction of cancer.[24] On the other hand, aliphatic poly(urethane-amine) (PUA), which shows distinct pH- and thermal-dual responsive property, has been used as the smart element in the present study.[25–27] The thermal-responsiveness of PUA is more biocompatible, and the preparation is simple and nontoxic.[4] AuNPs aggregates can effectively convert NIR light into heat and due to its thermally induced reversible transition property in aqueous solution above its lower critical solution temperature (LCST).[28] The amine group of PUA would change to the protonated amino forms with the decrease of pH value, which results in the pH-sensitivity of aliphatic PUA (see Supporting Information Figure S1).

In this article, hollow PUA/sodium poly(styrenesulfonate) (PSS)/Au microcapsules with NIR, pH, and temperature multiresponsive drug delivery properties have been prepared by LbL method. Hollow microcapsules could not enter the tissue interior and effectively avoid the aggregation and potential toxity of carriers within the tissue. Therefore, hollow microcapsule is a potent carrier for extracellular drug release. Moreover, compared with single-responsive nanocarriers with the size below 200 nm, it is more feasibe to endow the hollow microcapsules with multiple stimuli-responsiveness. As illustrated in Scheme 1, we chose $MnCO_3$ microparticles as template instead of others such as $CaCO_3$ microparticles, because $MnCO_3$ microparticles were easily redispersible after centrifugation and no apparent particle aggregation was observed during the process.[29] Aliphatic PUA and PSS were adsorbed onto the $MnCO_3$ template by LbL technique. Then, AuNPs aggregates were embedded onto the microparticles via the electrostatic interaction. Finally, hollow PUA/PSS/Au microcapsules were easily obtained by removing the $MnCO_3$ cores with ethylenediaminetetraacetic acid (EDTA).

AuNPs aggregates in the microcapsule shell endow the microcapsules with distinct NIR-responsive drug release property. Thanks to the electrostatic interaction variation between PUA and PSS at different pH conditions and the shrinkage of aliphatic PUA above its LCST, the prepared hollow microcapsules exhibited distinct pH- and thermal-dependent properties as illustrated in Scheme 1. More interestingly, we had discovered that the microcapsule morphology and the corresponding NIR-responsive drug release are strongly dependent on the pH value and temperature of the media. The possible interaction mechanism among different stimuli had also been discussed in the present article.

EXPERIMENTAL

Materials

Sodium poly(styrenesulfonate) (PSS, $M_w = 70{,}000$, Alfa Organics, China), doxorubicin hydrochloride (DOX, Beijing Huafenglianbo Chemical, China), manganese sulfate ($MnSO_4$, Tianjin Chemical Reagent Factory, China), ammonium bicarbonate (NH_4HCO_3, Tianjin Hengxing Chemical, China), isopropyl alcohol (IPA, Tianjin Shengao Chemical, China), sodium hyaluronate (HA, Liuzhou Liuhua Chemical, China) and chloroauric acid tetrahydrate ($HAuCl_4{\cdot}4H_2O$, Sinopharm Chemical Reagent, China), disodium ethylenediaminetetraacetic acid (EDTA, Tianjin Chemical Reagent Factory, China) were analytical reagents and used as received. The aliphatic PUA was synthesized by the copolymerization of 2-methylaziridine with CO_2 as illustrated in Supporting Information Figure S1.[29] The LCST of aliphatic PUA is 50°C as measured by a temperature-variable UV–vis spectrometer. The urethane content calculated from elemental analyses is 41.86%. M_w and PDI of the aliphatic PUA are 1.2×10^4 and 1.67, respectively.

Preparation of Au Nanoparticles

The classic Frens' method was used to prepare AuNPs. Briefly, 20 mL of $HAuCl_4$ solution (0.25 mM) was brought to a boil, and then 0.2 mL of sodium citrate solution (0.189*M*) was quickly added to the boiling solution with vigorous stirring.

Boiling and stirring were continued for 15 min, the heat source was then removed and the stirring was continued for an additional 15 min until the temperature reduced to room temperature. The resulting solution of colloidal particles was stored in the dark at 4°C for the later use.

Preparation of Hollow PUA/PSS/Au Microcapsules

Porous $MnCO_3$ microparticles were prepared by rapid mixing of equal volume of NH_4HCO_3 and $MnSO_4$ aqueous solutions. Typically, $MnSO_4$ solution (100 mL, 0.016*M*, with 0.5% IPA) was rapidly poured into NH_4HCO_3 (100 mL, 0.16*M*, with 0.5% IPA) and 100 mg HA mixed solution under vigorous stirring at 50°C. After 15 min, the precipitated $MnCO_3$ microparticles were washed with distilled water for three times and collected by centrifugation.

Microcapsules were fabricated via LbL technique. Typically, $MnCO_3$ microparticles were alternately incubated in 2 mg mL^{-1} of PUA aqueous solutions (pH 6.5) and then 2 mg mL^{-1} of PSS aqueous solutions (pH 6.6) for 15 min under gentle shaking. Nonadsorbed PUA or PSS was removed by three repeated refine circles of centrifugation (2000 rpm, 2 min)/washing prior to the addition of the oppositely charged polyelectrolyte solution. To form AuNPs aggregates, 2 mL of NaCl (0.8*M*) and AuNPs solution were mixed for 2 min. After self-assembly of four bilayers of polyelectrolyte, AuNPs agglomerates were deposited on the microparticles via sorption. $MnCO_3$ cores were dissolved by incubating in EDTA solution (0.1*M*, pH 7.3) for two times, each for 30 min. Hollow $(PUA/PSS)_4$-Au microcapsules were then obtained, which were further washed with water for three times and collected by centrifugation.

Characterization of Hollow PUA/PSS/Au Microcapsules

High magnification morphology of the hollow microcapsules was imaged using a field emission scanning electron microscopy (FESEM, JEOL 7500F). The incorporation of AuNPs inside the hollow microcapsules was confirmed by means of energy dispersive X-ray spectrometer (EDX, INCA). The sample solutions were dropped on a silicon wafer until drying and the silicon wafer was coated with an ~100 Å layer of platinum before observation. Transmission electron microscopy (TEM) was performed using a Tecnai G2 20 emission electron microscope (FEI) at an operating voltage of 200 kV. Zeta-potential of the $MnCO_3$ template and multilayer microcapsules were measured in 0.025*M* of NaCl solution with a pH value of 6.0 by a Zeta-sizer (nano ZS90 Malvern Instruments) to study the LbL process. At least three measurements were performed for each sample and the average values are shown as resulting zeta-potential.

Drug Loading and *In Vitro* Release Studies of Microcapsules

The hollow microcapsules were added to 4 mL of DOX solution (0.5 mg mL^{-1}) over 12 h with gentle shaking at 30°C. Then, DOX-loaded samples were washed and collected by centrifugation for three times. The UV–visible spectrophotometer was used to measure the DOX content of the clear supernatant at 481 nm from a calibration curve recorded at the same condition. The loading DOX content in microcapsules will be measured by taking away the DOX content of clear supernatant from the feed drug content. The drug loading efficiency can be calculated by the percentage of loaded drug based on feed amount.

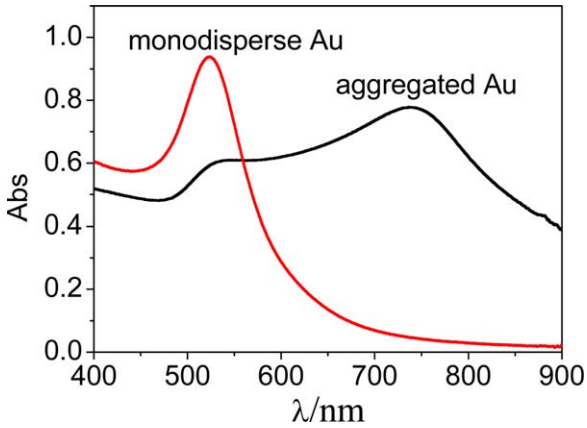

Figure 1. UV–Vis-NIR extinction spectra of monodisperse AuNPs and AuNPs aggregates (by adding 0.8*M* of NaCl solution for 2 min). [Color figure can be viewed in the online issue, which is available at wileyonlinelibrary.com.]

For the multiple-responsive drug release test, the DOX-loaded microcapsules were dispersed in a certain volume of PBS solution (pH = 7.4). Then, 1 mL of microcapsules was put in dialysis bags (cut-off MW 8000) with 3 mL release medium in different pH values (pH 2.1, 4.5, or 7.4), and then immersed in a conical flask of 26 mL release medium under continuously stirring at different temperatures (37 or 55°C). About 3 mL of sample was removed from the conical flask each hour and replaced by the same volume of fresh medium. A continuous wave (CW) laser source (780 nm, 120 mW) was employed to investigate the NIR-sensitivity of the microcapsules. The microcapsules were suspended in 2 mL of buffer solution (pH 4.5 or 7.4) with NIR irradiation at room temperature. 0.4 mL of sample was periodically removed and then diluted to 2 mL. An UV–visible spectrophotometer was used to analyze the amount of released drug. As a control test, microcapsules without NIR laser were analyzed using the same procedure.

RESULTS AND DISCUSSION

Aggregation of Au Nanoparticles

As shown by TEM image and the particle size distribution of AuNPs (Supporting Information Figure S2), the monodisperse AuNPs were spherical in shape with an average diameter of 20 nm and exhibited a narrow unimodal size distribution. As demonstrated by a Zeta-sizer instrument, the zeta-potential of AuNPs was around −16 mV. The relatively high negative charge made it possible for AuNPs to load into the hollow microcapsules via electrostatic interaction. The monodisperse AuNPs could not absorb NIR light, while AuNPs agglomerates could effectively absorb NIR light and convert light to heat. AuNPs agglomerates were generated by adding NaCl solutions to the monodisperse AuNPs solutions. NaCl solutions increased the ionic strength of AuNPs solutions, and then weakened the repulsion between the functional groups of AuNPs, leading to the accelerated accumulation of AuNPs.[24] AuNPs solutions rapidly changed from red to blue/grey and became unstable by adding 0.8*M* of NaCl solution for 2 min. Figure 1 shows the typical UV–Vis-NIR extinction spectra of monodisperse AuNPs and AuNPs aggregates. The corresponding absorption spectrum

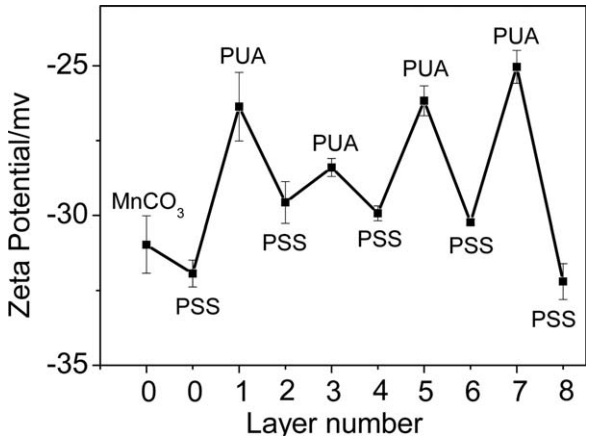

Figure 2. Evolution of zeta-potential during deposition of $(PUA/PSS)_4$ multilayers on the surface of $MnCO_3$.

displayed a new broad absorption region between 700 and 900 nm with a maximum absorption peak at 743 nm after aggregation, indicating the good absorption ability of AuNPs agglomerates at NIR area.

Characterization of Hollow PUA/PSS/Au Microcapsules

As mentioned above, we chose $MnCO_3$ microparticles as template because they were easily redispersible in aqueous solution after centrifugation.[27] Isopropanol (IPA) had been used as crystal growth additive to provide effective control over the crystallization process, leading to $MnCO_3$ crystals with desired size and dispersion.[30,31] Sodium hyaluronate (HA) was used to endow the $MnCO_3$ microparticles with negative charge. PSS had been adsorbed as the first layer to increase the negative charge of the template, which would improve the bonding force between $MnCO_3$ microparticles and polyelectrolyte.

Figure 2 shows the LbL self-assembly process by zeta-potential data. Negatively charged HA was used as crystal growth additive and endowed the $MnCO_3$ microparticles with negative charge. The zeta-potential of the HA-doped $MnCO_3$ microparticles was around −31 mV as illustrated in Figure 2. The zeta-potential changed to −32 mV after the assembly of PSS due to the strong negative charge of PSS. It could be seen that the zeta-potential was oscillated during the LbL self-assembly process, indicating that the polyelectrolyte multilayers were successfully assembled on the template.[32] In addition, the zeta-potential was overall negative even after the adsorption of PUA owing to the weak positive charge of PUA. It must be noted that the hollow multilayer microcapsules could be successfully obtained in spite of the overall negative zeta-potential during the self-assembling process. The hydrogen bonding between the sulfonic groups of PSS and the urethane groups of PUA contributed to the successful LbL self-assembly.[32,33]

As shown by Figure 3(A), the HA-doped $MnCO_3$ microparticles were spherical in shape with diameter of about 1–2 μm. Figure 3(D) shows a magnified FESEM image of $MnCO_3$ microparticles. It could be found that the surface of $MnCO_3$ microparticles was very coarse. After adsorption of the polyelectrolyte multilayers, the $MnCO_3$ template was dissolved by EDTA. Prior to laser irradiation, the microcapsules were spherical in solution but resembled deflated balloons after being dried for microscopic analysis [Figure 3(B)]. The magnified image [Figure 3(E)] showed that the surface of the polyelectrolyte microcapsules was relatively smooth compared with that of $MnCO_3$

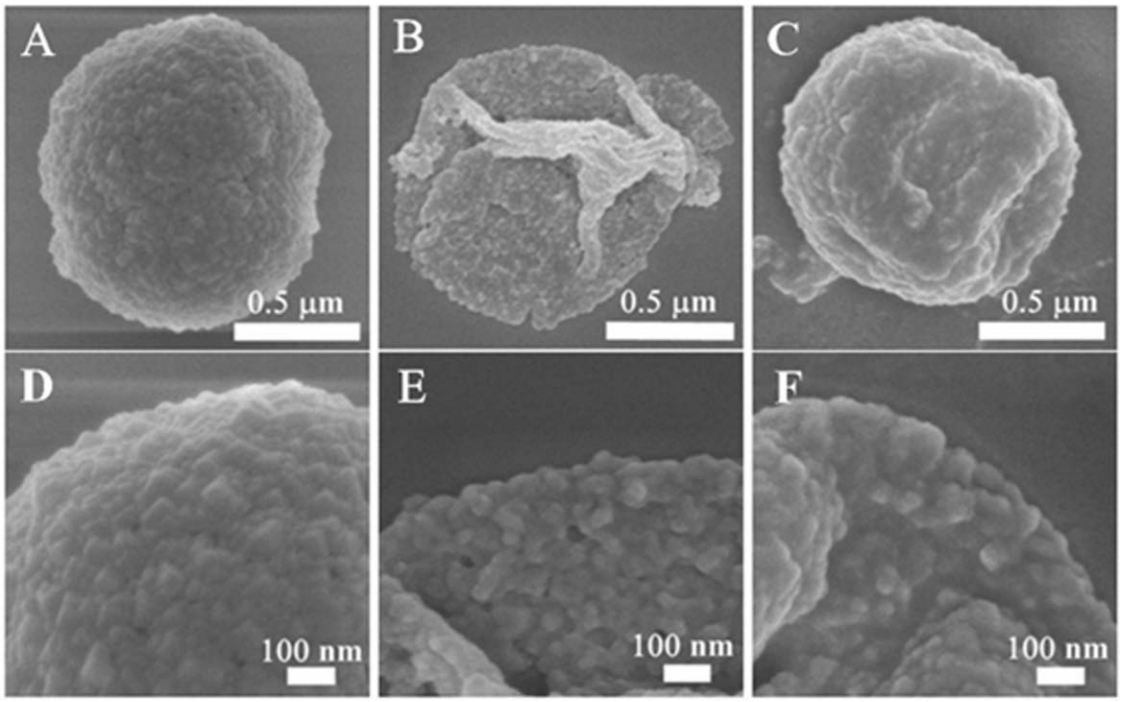

Figure 3. FESEM micrographs of $MnCO_3$ (A), hollow PUA/PSS/Au microcapsules before (B) and after NIR laser irradiation (C). (D), (E), (F) are the high magnification of (A), (B), (C), respectively.

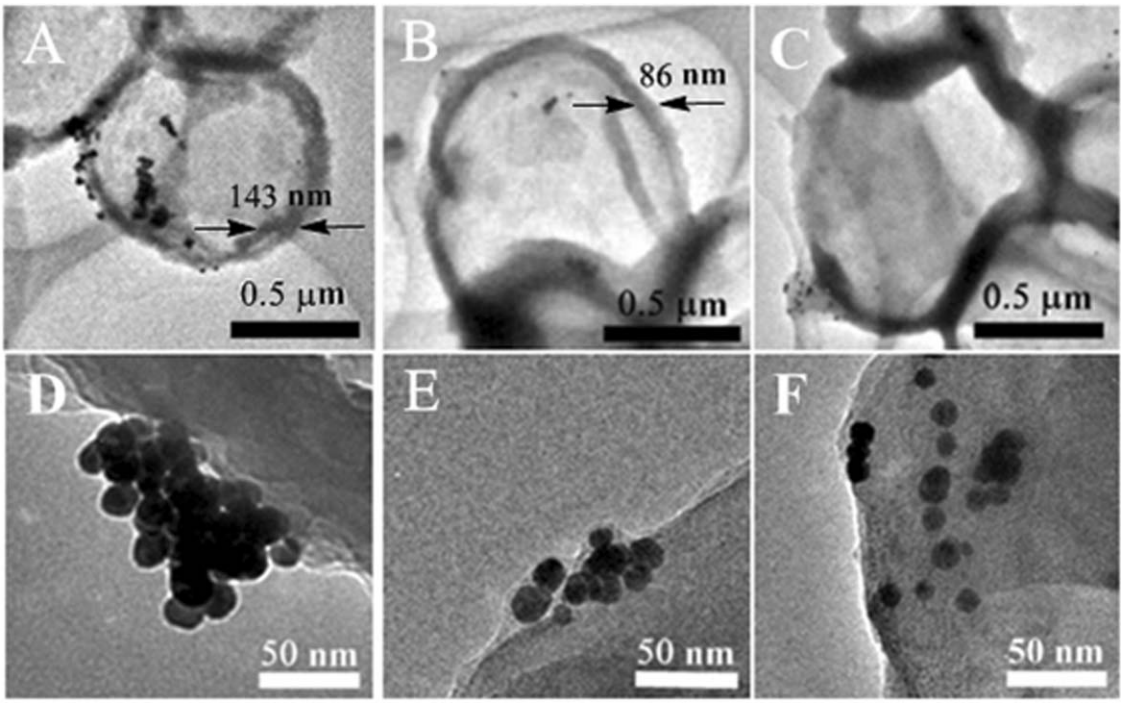

Figure 4. TEM images of hollow PUA/PSS/Au microcapsules before (A) and after NIR laser irradiation at pH 7.4 (B) and pH 4.5 (C). (D), (E), (F) are the high magnification of (A), (B), (C), respectively.

microparticles, indicating the incorporation of polyelectrolyte multilayers around the $MnCO_3$ template.[32] Figure 3(C) showed that the microcapsules shrunk upon NIR laser irradiation and the size of the microcapsules was smaller than that before the laser irradiation. It could also be observed from Figure 3(C) that the microcapsule shell was denser after NIR laser irradiation than that of original ones. AuNPs agglomerates could absorb NIR light and convert light energy to heat upon NIR laser irradiation, leading to a local temperature rise in the polyelectrolyte multilayers around the AuNPs.[24] When the local temperature became higher than the LCST of PUA, the polymer chains would shrink and ultimately obtain the smaller microcapsules with dense structure.[34] The EDX spectrum of hollow PUA/PSS/Au microcapsules (Supporting Information Figure S3) confirmed the presence of N element coming from aliphatic PUA and Au element deriving from AuNPs.

Figure 4 shows TEM images of hollow PUA/PSS/Au microcapsules before and after NIR laser irradiation at different pH values. The solid structure of multilayer $MnCO_3$ microparticles changed to hollow structure after dissolved by EDTA because of the disappearing of $MnCO_3$ core as demonstrated in Figure 4(A). It could also be observed that the thickness of the microcapsules shell was about 143 nm. Moreover, it could be clearly found from a magnified image of the microcapsule [Figure 4(D)] that the agglomerates AuNPs were embedded on the microcapsule shell. It could be observed in Figure 4(B) that after NIR laser irradiation at pH 7.4, the microcapsules kept intact but the thickness of the microcapsule shell decreased to around 86 nm, which was smaller than that before laser irradiation [Figure 4(A)]. The size decreasing of hollow microcapsules is perhaps derived from the shrinkage of the PUA and the local temperature rise in polyelectrolyte multilayers.[28] Figure 4(C) showed that after NIR laser irradiation at pH 4.5, microcapsules were partially damaged and intact microcapsules could not be observed. The possible reason is that more and more amino group of aliphatic PUA is protonated with decreasing pH value. Therefore, the electrostatic interaction between PSS and PUA is weakened, resulting the formation of fragile polyelectrolyte multilayers.[25,27] However, it could be observed that the aggregated AuNPs were melted and became smaller after NIR irradiation at pH 7.4 and 4.5 [Figure 4(E,F)]. The results suggested that the aggregated AuNPs had absorbed NIR light and converted light energy to heat.[24]

pH-/thermal-Sensitive Release

The prepared hollow microcapsules had better stability in aqueous solution. The static aqueous suspension of the studied microcapsules would be slowly deposited after several hours. However, after gentle shaking, slightly deposited hollow microcapsules would be redispersed in aqueous solution with the perfect shape. The drug loading efficiency of the hollow PUA/PSS/AuNPs microcapsules was 48.8%. Figure 5(A) shows the pH-dependent release of DOX from the hollow PUA/PSS/Au microcapsules at 37°C over a period of 24 h. As illustrated in Figure 5(A), DOX release increased with decreasing pH value from 7.4 to 2.1. Only 31.1% of DOX were released at pH 7.4 over 24 h, but almost 58.6% of DOX were released at pH 2.1 with the same treatment. Moreover, about 50% of DOX were released at pH 2.1 within the first 4 h. Scheme 1 clearly indicated that the hollow microcapsules had undergone the distinct structural change in acidic solution. With decreasing pH value, more and more amino groups of positive aliphatic PUA are protonated and the electrostatic repulsion between the positive charges

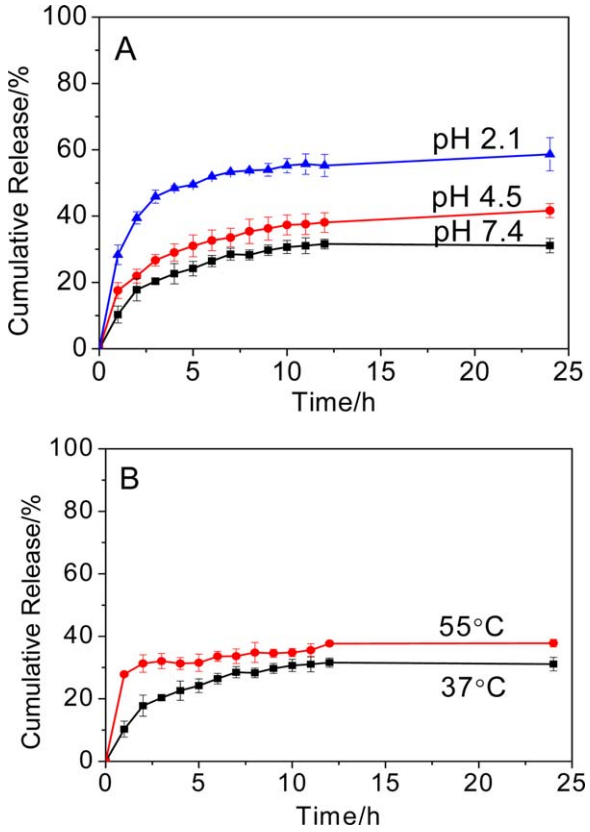

Figure 5. pH-dependent at 37°C (A) and thermal-dependent at pH 7.4 (B) release profiles of the hollow PUA/PSS/Au microcapsules. [Color figure can be viewed in the online issue, which is available at wileyonlinelibrary.com.]

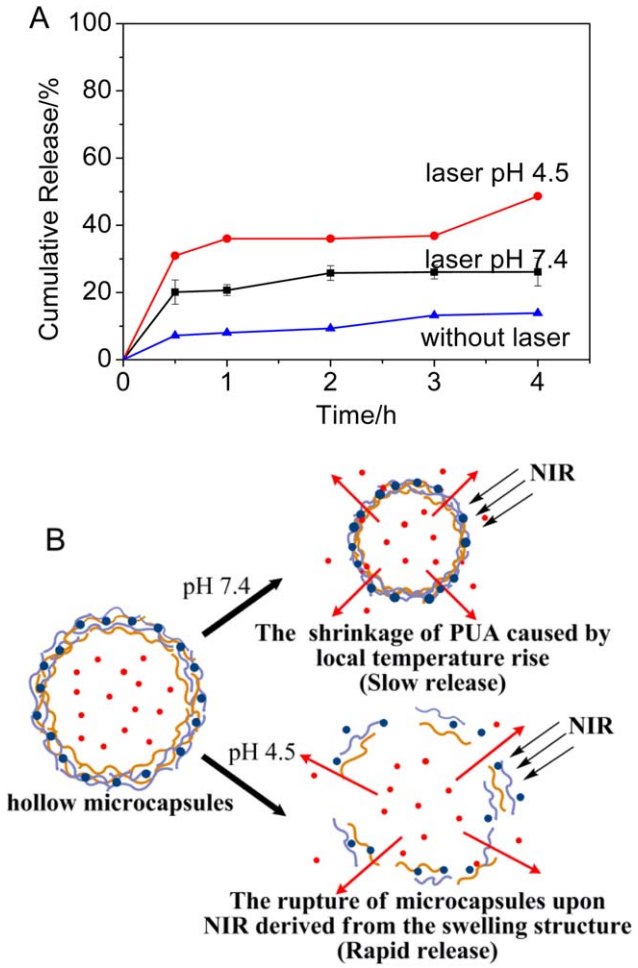

Figure 6. DOX release profiles of hollow PUA/PSS/Au microcapsules at pH 7.4 or 4.5, with or without NIR laser irradiation (A) and the schematic illustration of interdependent NIR/pH/temperature multi-sensitivity for hollow PUA/PSS/Au microcapsules (B). [Color figure can be viewed in the online issue, which is available at wileyonlinelibrary.com.]

results in a swelling structure.[25,26] Therefore, the polyelectrolyte walls would gradually loose and collapse to facilitate the rapid release of DOX.[35–37] It should also be noted that the total released DOX amount were relatively low for all studied pH conditions. The possible reason to this phenomenon is that the AuNPs inside the microcapsule shell probably increase the strength of the microcapsules, which results in the relatively lower drug release rate. The *P* value obtained from Student's *t* test analysis in the comparison between the release at pH 7.4 and 2.1 was <0.0001, the *P* value between the release at pH 7.4 and 4.5 were 0.0042. Both of the differences were very statistically significant (>95% confidence).

Figure 5(B) presents the thermal-responsive release profiles of hollow PUA/PSS/Au microcapsules at pH 7.4. As illustrated in experimental section, the LCST of aliphatic PUA employed in the present study was 50°C.[32] Therefore, we chose 37°°C, which was lower than the LCST; and 55°C, which was higher than the LCST, as the temperature conditions in smart drug delivery study. Compared with the release performance at 37°C, a distinct burst release was clearly observed at 55°C within the first 1 h for the hollow PUA/PSS/Au microcapsules. As illustrated in Scheme 1, when the temperature exceeds the LCST of PUA, polymer chains become contractive and DOX molecules would be squeezed from the hollow microcapsules and the rapid DOX release would be observed.[30,31] However, with the increasing of the shrinkage degree of the aliphatic PUA polymer chains, the polyelectrolyte multilayers become too dense to release the DOX.[32,33] Therefore, the release curve becomes relatively gentle after 2 h. The *P* value between the release at 55 and 37°C was 0.0441. The difference between these data was statistically significant (>95% confidence).

Interdependent NIR/pH/Temperature multi-Sensitivity

AuNPs aggregates could absorb NIR light and effectively convert light to heat, which have been widely used in thermotherapy by local laser irradiation.[24] As we know, the pH value of tumor is weak acid and the pH value of normal tissue is nearly neutral. Therefore, the investigation of NIR-responsiveness of the hollow microcapsules at different pH conditions is significant. To investigate the NIR-responsive release of DOX-loaded PUA/PSS/Au microcapsules at different pH conditions, a CW diode laser with a centre wavelength of 780 nm was employed.[36] It should be noted that the NIR-responsive drug release behaviour was performed at a static state in buffer solution with pH 7.4 and 4.5 [see Figure 6(A)]. It was different from the experiment

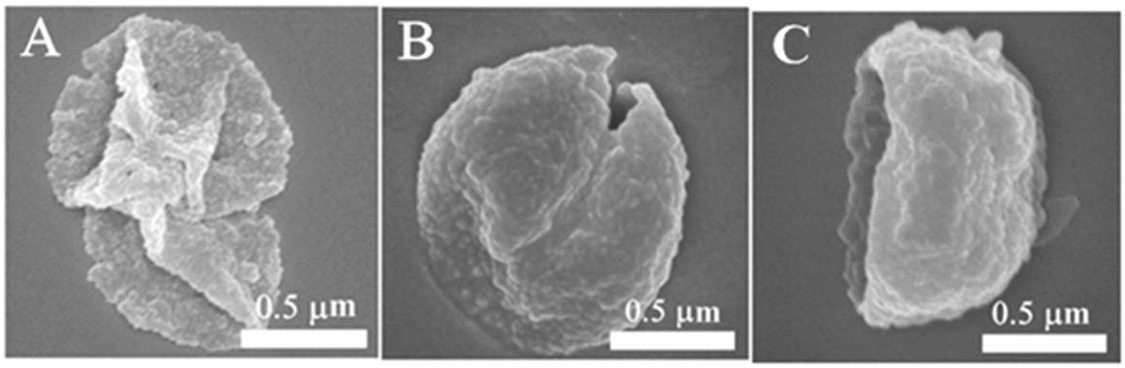

Figure 7. FESEM micrographs of hollow PUA/PSS/Au microcapsules before (A) and after NIR laser irradiation at pH 7.4 (B) and pH 4.5 (C).

condition of Figure 5, which was performed at a shaking bath. For the sample without the NIR laser irradiation, only 13.9% DOX were released within 4 h at pH 7.4. However, for the sample upon NIR laser irradiation at pH 7.4, the release of DOX already reached 20% within 30 min. It also can be observed from Figure 6(A) that the cumulative DOX release reached 48.6% within 4 h for the sample with the NIR laser irradiation at pH 4.5, which was significantly higher than that irradiated at pH 7.4 (20%) and without NIR irradiation (13.9%). Student's *t* test analysis showed that the difference between the release of hollow PUA/PSS/Au microcapsules without laser at pH 7.4 and with laser at pH 4.5 was very statistically significant (*P* value was 0.0088, >95% confidence).

The results indicated that the NIR-responsive drug release property was dependent on the media pH value. To confirm this conjecture, FESEM micrographs of hollow PUA/PSS/Au microcapsules before and after NIR laser irradiation at pH 7.4 and 4.5 were presented in Figure 7. It could be found that the microcapsule was integral before NIR laser irradiation and the microcapsule shell was soft and loose. Upon NIR laser irradiation at pH 7.4, the hollow microcapsules were partially damaged [Figure 4(B)]. The possible reason to this phenomenon is that the electrostatic interaction between PSS and PUA is strong at pH 7.4 and the heat energy generated by AuNPs aggregates could not destroy the polyelectrolyte multilayers substantially.[16,17,28,30] When the local temperature becomes higher than the LCST of PUA, the polymer chains would crinkle and ultimately lead to the shrinkage of the whole microcapsules. As a result, the microcapsules shell becomes dense [Figure 7(B)] and obstructs the drug release in the late [Figure 6(A)].[32,33] This phenomenon indicates that the NIR-responsiveness of hollow microcapsules is also related to the temperature. On the other hand, the microcapsule shell became dense for the sake of the local temperature rise upon NIR laser irradiation at pH 4.5 [Figure 7(C)], which was similar with the phenomenon at pH 7.4. However, it must be noted that the microcapsules had been damaged and could not keep the intact structure at pH 4.5 [Figure 7(C)]. At pH 4.5, the amino groups of positive aliphatic PUA are protonated and the electrostatic repulsion between the positive charges obstructs the interaction between aliphatic PUA and PSS.[25–27] Therefore, the microcapsule wall would undergo a transition from a continuous morphology to a nanoporous one deriving from the decrease of the electrostatic interaction between aliphatic PUA and PSS. The porous and unstable structure at weak acid condition is easy to be damaged upon the NIR laser irradiation. As a result, relatively rapid DOX release could be observed from the hollow microcapsules as illustrated in Figure 6(A).

The *in vitro* drug release investigation demonstrated that the NIR-effect at different pH values would produce different thermal-effect. The obtained hollow PUA/PSS/Au microcapsules exhibited multiple-responsive (NIR/pH/temperature) release properties. The microcapsule morphology and the corresponding NIR-responsive drug release were strongly dependent on the pH value and temperature of the media. In other words, the multiple stimuli were mutually interacted and interdependent. Therefore, the studied microcapsules have the potential to be used as a novel smart vehicle for remotely controlled multi-responsive drug delivery.

Drug Release Kinetics

The kinetics study of drug release could help us to better understand the drug release mechanism, which is very important to discover the relationship between the micro-morphology and multiple-responsiveness of the hollow microcapsules. To study the DOX release kinetics from hollow PUA/PSS/Au microcapsules, the DOX release data was fitted using the following empirical equation[38]:

$$\frac{M_t}{M_\infty} = kt^n \quad (1)$$

Here, M_t is the cumulative released mass of DOX at any time t; M_∞ is the total amount of the DOX in the microcapsules; k is release rate constant, and n is the diffusion exponent relating to the release mechanism. The DOX release kinetics of the microcapsules at different conditions was analyzed and the values of k, n and correlation coefficient (R^2) are shown in Supporting Information Table SI. It could be found that the n values ranged from 0.130 to 0.513, indicating that the drug release mechanism was Fickian diffusion or anomalous transport at these experiment conditions.

To accurately analyse the kinetics of DOX release from the hollow microcapsules, the n values were further determined from the slope of the $\ln(M_t/M_\infty)$ plot versus $\ln t$ according to eq. (1).

Supporting Information Figure S4(A) shows the curves of $\ln(M_t/M_\infty)$ versus ln$t$ for PUA/PSS/Au microcapsules at different pH values and temperatures. The n values of the microcapsules at pH 2.1 and 37°C ranged from 0.659 to 0.308 and produced a shift from anomalous transport to Fickian diffusion. It was related to the swelling of microcapsules at pH 2.1. The n values at pH 4.5 (37°C), pH 7.4 (37°C), and pH 7.4 (55°C) ranged from 0.998 to 0.312, from 0.893 to 0.321 and from 0.992 to 0.122, respectively, indicating a shift from Case-II transport to Fickian diffusion. Obviously, Case-II transport is the controlling mechanism when macromolecular relaxations predominate during the drug release process.[39,40] The possible reason to this phenomenon is that the swelling/shrink of the polyelectrolyte multilayers only happened at the early stage of drug release, and later the DOX release is mainly derived from the molecular free diffusion.

Supporting Information Figure S4(B) shows the curves of $\ln(M_t/M_\infty)$ versus ln$t$ for PUA/PSS/Au microcapsules with and without NIR laser at different pH values. The n values of the microcapsules with NIR laser at pH 4.5 ranged from 0.112 to 0.496 and produced a shift from Fickian diffusion to anomalous transport. The possible reason for this phenomenon is that AuNPs agglomerates have changed light to heat upon NIR laser irradiation, and the local temperature rise leads to the polymer relaxation. The n values of the microcapsules with NIR laser at pH 7.4 ranged from 0.267 to 0.018, indicating that the DOX release mechanism was Fickian diffusion. In addition, it could also be found from Supporting Information Figure S3(B) that the n value of the microcapsules without NIR laser ranged from 0.189 to 0.574, indicating a shift from Fickian diffusion to anomalous transport, which related to the water transport mechanism.[39] The above analysis results demonstrated that the DOX release kinetics was significantly affected by release media for hollow PUA/PSS/Au microcapsules.

CONCLUSIONS

Multiresponsive hollow microcapsules made of aliphatic PUA, PSS, and AuNPs have been prepared via LbL technique in the present article. Hollow microcapsules exhibit obvious pH- and thermal-dependent property for the sake of the shrinkage of PUA above its LCST and the interaction variation between PUA and PSS at different pH conditions. The AuNPs aggregates inside the microcapsules can effectively convert light to heat upon irradiation with NIR laser and endow the hollow microcapsules with distinct NIR-responsiveness. More importantly, we have discussed the possible interaction mechanism about the interdependent NIR-, pH-, and thermal-responsive properties of the hollow microcapsules. The results suggest that the studied hollow microcapsules can be used as a novel smart microcarrier for remotely controlled multi-responsive drug delivery.

ACKNOWLEDGMENTS

This work was supported by grants from the National Natural Science Foundation of China (Projects 20874090 and 21074119).

REFERENCES

1. Lapeyre, V.; Renaudie, N.; Dechezelles, J. F.; Saadaoui, H.; Ravaine, S.; Ravaine, V. *Langmuir* **2009**, *25*, 4659.
2. Zhang, J.; Xu, X. D.; Liu, Y.; Liu, C. W.; Chen, X. H.; Li, C.; Zhuo, R. X.; Zhang, X. Z. *Adv. Funct. Mater.* **2012**, *22*, 1704.
3. Zhang, J. F.; Chen, D. D.; Li, Y.; Sun, J. Q. *Polymer* **2013**, *54*, 4220.
4. Romero, S. C.; Ochs, M.; Gil, P. R.; Ganas, C.; Pavlov, A. M.; Sukhorukov, G. B.; Parak, W. J. *J. Controlled Release* **2012**, *159*, 120.
5. Viger, M. L.; Sheng, W. Z.; Dore, K.; Alhasan, A. H.; Carling, C. J.; Lux, J.; Lux, C. G.; Grossman, M.; Malinow, R.; Almutairi, A. *ACS Nano* **2014**, *8*, 4815.
6. Wu, Y. J.; Lin, X. K.; Wu, Z. G.; Mohwald, H.; He, Q. *ACS Appl. Mater. Interfaces* **2014**, *6*, 10476.
7. Hu, B.; Zhang, L. P.; Chen, X. W.; Wang, J. H. *Nanoscale* **2013**, *5*, 246.
8. Jiang, Y.; Zeng, F.; Gong, R. Y.; Guo, Z. X.; Chen, C. F.; Wan, X. B. *Soft Matter* **2013**, *9*, 7538.
9. Yuan, Q. C.; Cayre, O. J.; Fujii, S.; Armes, S. P.; Williams, R. A.; Biggs, S. *Langmuir* **2010**, *26*, 18408.
10. Berger, S.; Zhang, H. P.; Pich, A. *Adv. Funct. Mater.* **2009**, *19*, 554.
11. Cheng, Y.; Doane, T. L.; Chuang, C. H.; Ziady, A.; Burda, C. *Small* **2014**, *10*, 1799.
12. Cao, Z. H.; Landfester, K.; Ziener, U. *Langmuir* **2012**, *28*, 1163.
13. Loretta, L. M.; Marzia, M. F.; Francesca, B. *Adv. Colloid Interface Sci.* **2014**, *207*, 139.
14. Budhlall, B. M.; Marquez, M.; Velev, O. D. *Langmuir* **2008**, *24*, 11959.
15. Jin, Y. S.; Wang, J. R.; Ke, H. T.; Wang, S. M.; Dai, Z. F. *Biomaterials* **2013**, *34*, 4794.
16. De Koker, S.; Hoogenboom, R.; De Geest, B. G. *Chem. Soc. Rev.* **2012**, *41*, 2849.
17. Bédard, M. F.; Braun, D.; Sukhorukov, G. B. *ACS Nano* **2008**, *2*, 1807.
18. Angelatos, A. S.; Radt, B.; Caruso, F. *J. Phys. Chem. B* **2005**, *109*, 3071.
19. Shi, W. L.; Sahoo, Y.; Swihart, M. T.; Prasad, P. N. *Langmuir* **2005**, *21*, 1610.
20. Shi, P.; Ju, E. G.; Ren, J. S.; Qu, X. G. *Adv. Funct. Mater.* **2014**, *24*, 826.
21. Jeong, W. C.; Kim, S. H.; Yang, S. M. *ACS Appl. Mater. Interfaces* **2014**, *6*, 826.
22. Lee, B.; Kim, H. S.; Kim, J. *Chem. Commun.* **2013**, *49*, 1865.
23. Pissuwan, D.; Valenzuela, S. M.; Miller, C. M.; Cortie, M. B. *Nano Lett.* **2007**, *7*, 3808.
24. Ji, X. H.; Song, X. N.; Li, J.; Bai, B. Y.; Yang, W. S.; Peng, X. G. *J. Am. Chem. Soc.* **2007**, *129*, 13939.
25. Ihata, O.; Kayaki, Y.; Ikariya, T. *Chem. Commun.* **2005**, *17*, 2268.

26. Li, G. F.; Liu, Y. L.; Zhang, K.; Shi, J.; Wan, X.; Cao, S. K. *J. Appl. Polym. Sci.* **2013**, *129*, 3696.
27. Shi, J.; Shi, J.; Du, C.; Chen, Q.; Cao, S. K. *J. Membr. Sci.* **2013**, *433*, 39.
28. Gu, L.; Wang, X. H.; Chen, X. S.; Zhao, X. J.; Wang, F. S. *J. Polym. Sci. A* **2011**, *49*, 5162.
29. Zhu, Y.; Tong, W. J.; Gao, C. Y.; Mohwald, H. J. *Mater. Chem.* **2008**, *18*, 1153.
30. Zhu, H. G.; Stein, E. W.; Lu, Z. H.; Lvov, Y. M. *Chem. Mater.* **2005**, *17*, 2323.
31. Ma, Y. J.; Dong, W. F.; Kooij, E. S.; Hempenius, M. A.; Mohwald, H.; Vancso, G. J. *Soft Matter* **2007**, *3*, 889.
32. Du, C.; Shi, J.; Zhang, L.; Cao, S. K. *Mater. Sci. Eng. C* **2013**, *33*, 3745.
33. Kozlovskaya, V.; Kharlampieva, E.; Drachuk, I.; Cheng, D.; Tsukruk, V. V. *Soft Matter* **2010**, *6*, 3596.
34. Shi, J.; Du, C.; Shi, J.; Wang, Y. M.; Cao, S. K. *Macromol. Biosci.* **2013**, *13*, 494.
35. Alizadeh, R.; Ghaemy, M. *Polymer* **2015**, *66*, 179.
36. Xu, S. H.; Shi, J.; Feng, D. S.; Yang, L.; Cao, S. K. *J. Mater. Chem. B* **2014**, *2*, 6500.
37. Shi, J.; Qi, W. Y.; Du, C.; Shi, J.; Cao, S. K. *J. Appl. Polym. Sci.* **2013**, *129*, 577.
38. Ritger, P. L.; Peppas., N. A. *J. Controlled Release* **1987**, *5*, 37.
39. Khare, A. R.; Peppas, N. A. *Biomaterials* **1995**, *16*, 559.
40. Yang, L.; Shi, J.; Zhou, X. F.; Cao, S. K. *Int. J. Biolog. Macrom.* **2015**, *73*, 1.